




Identifying Abelian and non-Abelian topological orders in the string-net model using a quantum scattering circuit

Ze Zhang ^{1,*}, Xinyue Long,^{1,*} Xiuzhu Zhao,¹ Zidong Lin,¹ Kai Tang,¹ Hongfeng Liu,¹ Xiaodong Yang,¹ Xinfang Nie,^{1,2} Jiansheng Wu ^{1,2}, Jun Li,^{1,2} Tao Xin,^{1,2,†} Keren Li,^{3,1,‡} and Dawei Lu ^{1,4,2,§}

¹Shenzhen Institute for Quantum Science and Engineering and Department of Physics, Southern University of Science and Technology, Shenzhen 518055, China

²Guangdong Provincial Key Laboratory of Quantum Science and Engineering, Shenzhen 518055, China

³Peng Cheng Laboratory, Shenzhen 518066, China

⁴Shenzhen Key Laboratory of Advanced Quantum Functional Materials and Devices, Southern University of Science and Technology, Shenzhen 518055, China



(Received 30 September 2021; accepted 11 March 2022; published 29 March 2022)

Realizing universal topological quantum computers requires the manipulation of non-Abelian topological orders in a physical system, which presents great challenges. Conversely, the rapid development in circuit-based quantum computing offers a reliable quantum simulation approach to study these topological orders. The preliminary problem is how to identify distinct topological orders. Here, we develop a framework based on the quantum scattering circuit to directly and efficiently measure the modular transformation matrix, which is widely deemed as the fingerprint of a given topological order. The information of the modular transformation matrix is encoded in the probe qubit, and the readout merely requires single-qubit Pauli measurements. We further implement the scheme in a nuclear magnetic resonance quantum simulator to emulate the string-net model, where an Abelian \mathbb{Z}_2 toric code and a non-Abelian Fibonacci order emerge. In particular, the latter is predicted to be the simplest candidate for universal topological quantum computers. The two topological orders are unambiguously distinguished by the experimentally measured modular transformation matrices. As an experimental demonstration of a non-Abelian topological order with efficient readout, our work may open avenues toward investigating topological orders in circuit-based quantum simulators.

DOI: [10.1103/PhysRevA.105.L030402](https://doi.org/10.1103/PhysRevA.105.L030402)

Introduction. Beyond the Landau-Ginzburg symmetry-breaking paradigm, topological orders (TOs) describe different phases of matter with the same symmetry [1–7]. Such a TO system is immune to local perturbations and is thus a candidate for topological quantum computation (TQC) [8–11]. There are abundant phenomena in TOs, including degenerate ground states and quasiparticle excitations. Degenerate ground states can be used for quantum memories [12,13], and quasiparticle excitations can be used for quantum computation [8,9,14]. A non-Abelian TO provides an extraordinary route to build a fault-tolerant quantum computer; however, its physical realization remains a great challenge. One of the most promising candidates, Majorana fermions, has been overshadowed due to recent academic debates about its experimental evidence [15,16]. So, at this stage where moderate-scale quantum simulators are available, it is worth studying topological features of TO models using circuit-based quantum simulation. To achieve such goals, the prerequisite is to efficiently distinguish diverse TOs in experiment, which is the aim of this work.

The primary feature of a TO is the topology-protected ground-state degeneracy (GSD) [3,17,18]. Excited states and the corresponding quasiparticles (anyons) can be obtained by applying string operators on these degenerate ground states. Furthermore, the dynamics of anyons, including self-braiding and double-braiding, can be realized by applying string operators on the excited states [19]. The self-braiding dynamics, represented by self-statistical phase factors, is recorded by the T matrix. Meanwhile, the double-braiding dynamics, represented by mutual-statistical phase factors, is recorded by the S matrix [20,21]. The T and S matrices are called modular transformation matrices (MTMs). Since T and S matrices for each TO are unique, MTMs are widely deemed as the *fingerprints* of TOs, and hence, their measurements are important for TO characterization. In general, MTMs can be measured in a discrete model from ground-state wave-function overlap after appropriate transformations on the lattice, which is widely applied in numerical simulations to identify topological orders [22–26]. Moreover, these quantities can be related to complex experimental observables which can be extracted by quantum state tomography (QST). A problem arises: How do we measure the MTMs of a given TO in an efficient way? Here, efficiency means that the experimental cost for measurement should be polynomial with the growth of qubits, thus excluding the QST method. As simulating TOs inevitably handles degenerate ground states, QST is indeed a

*These authors contributed equally to this work.

†xint@sustech.edu.cn

‡likr@pcl.ac.cn

§ludw@sustech.edu.cn

straightforward way for extracting the information, but it is not efficient [27].

In this work, we design a quantum scattering circuit to perform efficient measurement of MTMs, where matrix elements are directly extracted. The model to be emulated is chosen as the string-net model on the minimal honeycomb lattice proposed by Levin and Wen [28], and the experimental platform is the nuclear magnetic resonance (NMR) quantum simulator. This model has two distinct TOs with the same GSD: The Abelian \mathbb{Z}_2 toric code and the non-Abelian doubled Fibonacci order [17,18,28,29]. Owing to the applications in TQC, simulating TOs is a long-term goal in various physical systems [19,27,30–38], while significant progress has been made this year in a 25-qubit superconducting system to simulate the toric code [39]. Apart from these previous experiments that focus on Abelian anyonic statistics [19,27,30–35], we experimentally study both the Abelian and non-Abelian TOs, and we identify them by measuring the combined MTM ST^{-1} [23]. As the *fingerprint* of a particular TO in the string-net model, ST^{-1} is directly measured via the ancilla-assisted scattering quantum circuit—an efficient method compared to QST [40,41]. The measured matrices for the Abelian and non-Abelian TOs are fundamentally different, while both of them have over 97% fidelity. So, the Abelian and non-Abelian TOs have been experimentally identified in a reliable and efficient way.

String-net model. A string-net model is defined on the honeycomb lattice, specified by its string types, fusion rules, and Hamiltonian [28,42]. The general form of the Hamiltonian is $H = -\sum_v A_v - \sum_p B_p$, where A_v is the star operator for each vertex v , and B_p is the plaquette operator for each plaquette p , as shown in Fig. 1(a). All the operators A_v and B_p commute with each other, rendering this model exactly solvable [9]. The minimal structure of this string-net model can be obtained by shrinking the honeycomb lattice onto a torus, with merely three strings, two vertices, and one plaquette [see Fig. 1(b)]. The three strings determine the Hamiltonian to be eight-dimensional, while it has three distinct forms because of the three possible sets of fusion rules [43]. Accordingly, there are three distinct TOs in this model.

The three TOs are the \mathbb{Z}_2 toric code, the doubled semion order, and the doubled Fibonacci order, respectively. The former two are Abelian, and the last one is non-Abelian, which is a potential candidate for universal TQC. These TOs cannot be simply distinguished by their GSD, as it is always fourfold. Nevertheless, the T and S matrices for each TO are unique, offering a potential approach to realize their identifications. Here, as the primary difference between the two Abelian orders is just the anyon type (fermionic with statistics -1 or semionic with statistics i), we only consider the \mathbb{Z}_2 toric code in the remainder of this work.

The T and S matrices are described by the self- and mutual-statistical theorems, respectively. In the \mathbb{Z}_2 toric code, there are four species of anyons: 1 , e , m , and ϵ . The first three are bosons, while the ϵ quasiparticle is a fermion [44,45]. Therefore, when circling the four anyons around themselves, the self-statistical phase factors would constitute the T matrix: $T = \text{Diag}\{1, 1, 1, -1\}$. When moving an anyon around the others, novel phase factors like -1 will be obtained. These

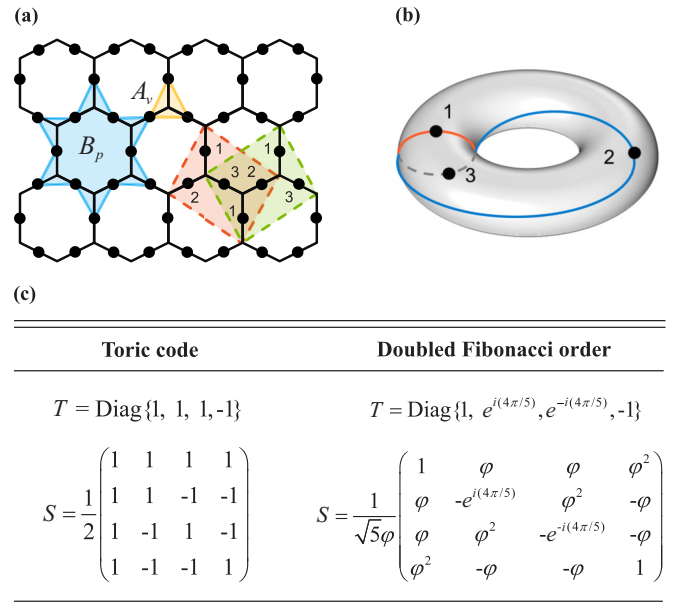


FIG. 1. (a) String-net model on a honeycomb lattice. A_v and B_p are the vertex (yellow) and plaquette (blue) operators, respectively. The unit cell of the minimal string-net model with periodic boundary conditions is shown by the green region, which consists of three strings labeled by 1, 2, and 3. This unit cell is equivalent to the torus structure in panel (b). The combined MTM ST^{-1} can be realized by rotating the unit cell counterclockwise by $\pi/3$ to the red region. It is obvious that the rotation cyclically permutes the three strings by $1 \rightarrow 2 \rightarrow 3 \rightarrow 1$. (b) Minimal structure of the string-net model on a torus. (c) T and S matrices for the toric code and the doubled Fibonacci order. $\varphi = (1 + \sqrt{5})/2$ is the golden ratio.

mutual-statistical phase factors produce the S matrix, with the form in Fig. 1(c).

For the doubled Fibonacci order, the self-statistics is more nontrivial. There are also four types of anyons: 1 , τ , $\bar{\tau}$, and $\tau\bar{\tau}$. For τ and $\bar{\tau}$, the self-statistics is exotic because nontrivial phase factors, $e^{i(4\pi/5)}$ or $e^{-i(4\pi/5)}$, will be observed. The T matrix is thus $T = \text{Diag}\{1, e^{i(4\pi/5)}, e^{-i(4\pi/5)}, 1\}$. The anyon τ is called the Fibonacci anyon because the dimension of the Hilbert space of n τ 's grows as the Fibonacci sequence with n . The S matrix generated from mutual statistics is shown in Fig. 1(c), where $\varphi = (1 + \sqrt{5})/2$ is the golden ratio. To realize universal TQC, the Hilbert space of two Fibonacci anyons is two-dimensional and, hence, can be encoded as a logical qubit. Moreover, the non-Abelian braiding dynamics in this model is capable of generating universal quantum gates [43].

Identification protocol. As illustrated above, the sole way to identify TOs of the string-net model is by measuring their corresponding MTMs. It requires one to apply the modular transformation on the fourfold degenerate ground states and change the ground-state basis. However, for the case of honeycomb lattice on the torus, S and T matrices cannot be measured simultaneously. Cincio and Vidal show that a $\pi/3$ rotation of the lattice about the axis perpendicular to the lattice surface leads to a combined modular transformation ST^{-1} , which can be used to identify TOs as well [23]. The $\pi/3$

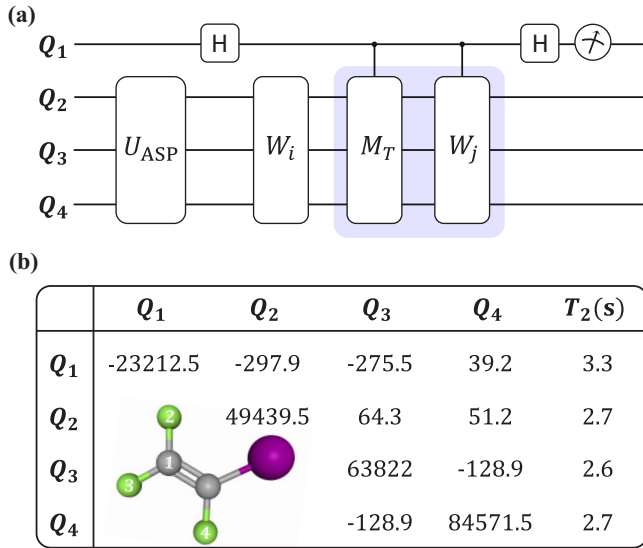


FIG. 2. (a) Quantum scattering circuit for identifying TOs. The combined MTM ST^{-1} can be obtained by measuring $\langle\sigma_z\rangle$ and $\langle\sigma_y\rangle$ of the probe qubit. The initial state is $|0000\rangle$, and the function of each operator is described in the main text. The operator $U = W_j M_T$ marked by blue is the target that needs to be scattered. (b) Molecule structure of the ^{13}C -iodotrifluoroethylene, where one ^{13}C (gray, Q_1) and three ^{19}F 's (green, Q_2 to Q_4) form a four-qubit system. The table lists the parameters of chemical shifts (diagonal, Hz), J -coupling strengths (off diagonal, Hz), and T_2 relaxation times.

rotation for this honeycomb structure is equivalent to a cyclic permutation among the three strings ($1 \rightarrow 2 \rightarrow 3 \rightarrow 1$), as shown in Fig. 1(a). This permutation can be realized by an operator M_T consisting of two SWAP gates for $1 \leftrightarrow 2$ and $2 \leftrightarrow 3$, making it executable by quantum circuits.

The quantum circuit for measuring the ST^{-1} matrix is shown in Fig. 2(a). It contains one probe qubit Q_1 for detection and three system qubits (Q_2 to Q_4) to emulate the string-net model. Let us start from the system qubits, which are initialized to $|000\rangle$. For a given TO model, the first step is to prepare its four degenerate ground states. This degeneracy prohibits the usage of traditional adiabatic passages, but one can employ the random preparation of the linearly independent ground states approach [35], labeled by U_{ASP} . From $|000\rangle$, the system is prepared into a particular ground state by U_{ASP} , and a subsequent string operator W_i ($1 \leq i \leq 4$) is applied to evolve this ground state to all four degenerate ground states $|\phi_i\rangle$ in the original basis. The ST^{-1} modular transformation, marked by M_T in Fig. 2(a), changes the ground-state basis by $|\psi_i\rangle = M_T|\phi_i\rangle$. Here, M_T is a concatenation of two SWAP gates. The final block W_j ($1 \leq j \leq 4$) is similar to W_i , which traverses $|\psi_i\rangle$ to all four ground states $|\psi_j\rangle$ in the new basis.

The ST^{-1} matrix is reconstructed by inner products of the ground states before and after the basis change. Explicitly, each element in the ST^{-1} matrix is a complex number, calculated by $ST_{ij}^{-1} = \langle\phi_i|\psi_j\rangle$, where $1 \leq i, j \leq 4$. By combining M_T and W_j as $U = W_j M_T$, we can rewrite the matrix element as

$$ST_{ij}^{-1} = \langle\phi_i|\psi_j\rangle = \langle\phi_i|U|\phi_i\rangle = \text{Tr}(U|\phi_i\rangle\langle\phi_i|). \quad (1)$$

Here, $|\phi_i\rangle$ and $|\psi_j\rangle$ are the fourfold degenerate ground states in the original and new bases, respectively.

The measurement of $\text{Tr}(U\rho)$, where $\rho = |\phi_i\rangle\langle\phi_i|$, can be efficiently realized using the quantum scattering circuit [41]. The scattering circuit, as an analog to the classical scattering experiment, plays an important role in many algorithms [40,41,46–51]. It can be adapted as a tomographer by extracting information on the operator U with a known state ρ , or as a spectrometer by learning the state ρ with some specific U 's. As shown in Fig. 2(a), we first initialize the probe qubit Q_1 to $|0\rangle$ and apply a Hadamard gate to create its equal-superposition state. The two controlled operations do nothing if the probe is in $|0\rangle$, but apply the labeled unitary operator if the probe is in $|1\rangle$. After applying another Hadamard gate on the probe, its two Pauli observables have remarkable properties:

$$\langle\sigma_z\rangle = \text{Re}[\text{Tr}(U\rho)], \quad \langle\sigma_y\rangle = -\text{Im}[\text{Tr}(U\rho)]. \quad (2)$$

So we can measure ST^{-1} via Eqs. (1) and (2) without QST and acquire the *fingerprints* of the TO efficiently.

Experiment. We perform the quantum simulation of the Abelian \mathbb{Z}_2 toric code and the non-Abelian doubled Fibonacci order using a four-qubit NMR quantum simulator. The experiments are carried out on a Bruker 600 MHz spectrometer. The processor is the ensemble of ^{13}C -iodotrifluoroethylene dissolved in d -chloroform [52–54] [see Fig. 2(b)]. The three ^{19}F spins are the system qubits (Q_2 to Q_4), and the ^{13}C spin is the probe in the scattering circuit. The corresponding Hamiltonian of this system is

$$H_{\text{NMR}} = -\sum_{i=1}^4 \frac{\omega_i}{2} \sigma_i^z + \sum_{i<j,=1}^4 \frac{\pi J_{i,j}}{2} \sigma_i^z \sigma_j^z, \quad (3)$$

where $\omega_i/2\pi$ is the Larmor frequency of the i th spin, and J_{ij} is the scalar coupling between the i th and j th spins. The parameters are listed in Fig. 2(b).

The processor is firstly initialized to $|0000\rangle$ by the spatial average pseudopure state-preparation technique with experimental fidelity over 0.99 [43]. The subsequent U_{ASP} on the system qubits represents a random quantum adiabatic passage, which in principle contains massive single-qubit and two-qubit gates. In experiment, as $|\phi_1\rangle = (|000\rangle + |011\rangle)/\sqrt{2}$ is a joint ground state for both the toric code and the doubled Fibonacci order, we adopt the regular state-preparation approach in simulating anyonic statistics [43], that is, by implementing a Hadamard gate on Q_3 and a CNOT₃₄ gate (Q_3 as the control and Q_4 as the target) to prepare it. Meanwhile, the probe qubit Q_1 is prepared to $(|0\rangle + |1\rangle)/\sqrt{2}$ by a 1-ms shaped pulse of $\pi/2$ rotation about the y axis, which is embedded in the state-preparation pulse during optimization [55,56].

The form of the loop operator $W_{i,j}$ depends on the corresponding TO. For the \mathbb{Z}_2 toric code, the operator is simply comprised of single-qubit rotations. For the doubled Fibonacci order, the form is highly complex; see the Supplemental Material [43]. In experiment, we utilize optimized pulses of the same length, 20 ms, to realize these loop operators, so that the decoherence errors for the two cases are comparable. The combined modular transformation M_T , which is actually a concatenation of two controlled-SWAP gates, has an extremely long sequence. So we optimize the

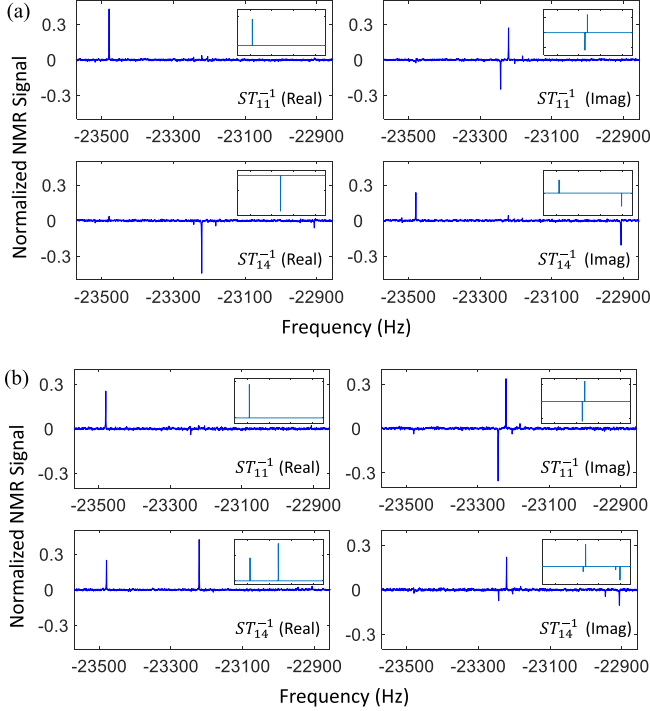


FIG. 3. NMR spectra of the probe qubit Q_1 for identifying (a) the toric code and (b) the doubled Fibonacci order. The experimental spectra are shown in blue, while the simulated ones are shown in insets. Here, for each model, a diagonal element ST_{11}^{-1} and an off-diagonal element ST_{14}^{-1} are shown. The real and imaginary parts correspond to the measurement of $\langle\sigma_z\rangle$ and $\langle\sigma_y\rangle$, respectively.

sequence via a compiler program and achieve a packed pulse of 25 ms [43]. The last step is to apply another 1-ms Hadamard gate on the probe qubit. The total length of the quantum circuit is 90 ms, which is less than 4% of the T_2 relaxation time.

As shown in Eq. (1), each element in the ST^{-1} matrix corresponds to the expectation values $\langle\sigma_z\rangle$ for the real part and $\langle\sigma_y\rangle$ for the imaginary part, of the probe qubit. In experiment, $\langle\sigma_y\rangle$ can be directly measured from the NMR spectra, while $\langle\sigma_z\rangle$ needs to be rotated to the transverse plane by a $\pi/2$ selective pulse before measurement. A least-square fitting program is used to extract the values from the spectra. Since the measurement is only performed on the probe qubit with simple operations, the errors in this readout stage is nearly ignorable. In Fig. 3, we plot the experimental NMR spectra for measuring the diagonal element ST_{11}^{-1} and the off-diagonal element ST_{14}^{-1} . The simulated spectra (insets) are also presented for comparison. It is clear that the simulations are in excellent accordance with the experimental results, indicating the accuracy of this scheme in TO identifications.

By repeatedly implementing the quantum scattering circuit in Fig. 2(a) with all loop operators $W_{i,j}$, we obtain the entire MTM ST^{-1} . The experimental results for the \mathbb{Z}_2 toric code and the doubled Fibonacci order are shown in Fig. 4. The results indicate that the matrices for these two TOs are widely dissimilar, manifesting that the two TOs are highly distinct. To quantitatively evaluate their overlap, we compute the p -norm

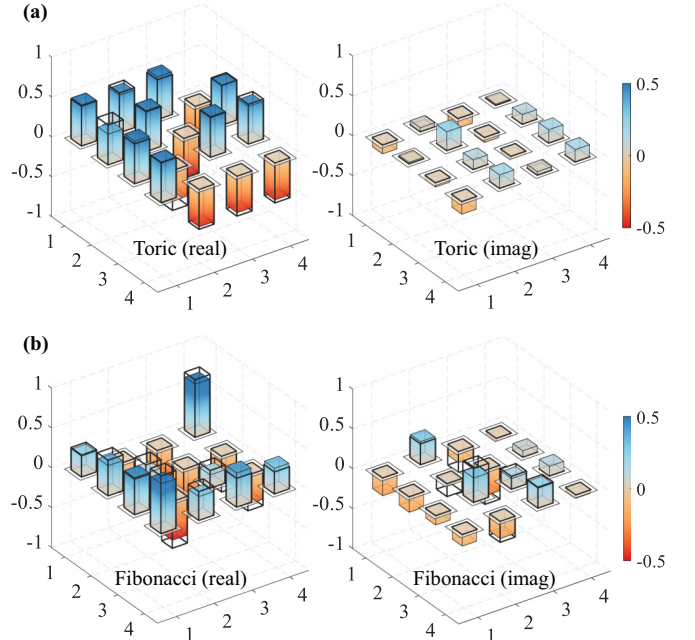


FIG. 4. Experimental ST^{-1} matrices for (a) the toric code and (b) the doubled Fibonacci order. The colored bars are the experimental results, and the outlines are the theoretical predictions.

deviation matrix by

$$C_p = \max\{\|(\mathcal{M}_1 - \mathcal{M}_2)\vec{x}\|_p : \vec{x} \in \mathbb{R}^4, \|\vec{x}\| = 1\}, \quad (4)$$

where \mathcal{M}_1 and \mathcal{M}_2 are the matrices to be distinguished, and a special case of $p = 2$ corresponds to the Euclidean distance. In experiment, the normalized Euclidean distance between the ST^{-1} matrices of the two TOs is 0.981, which is very close to their theoretical distance 0.979. In addition, we also calculate the average fidelity between the MTMs of the two TOs by $\bar{F}(\Lambda, \mathcal{U}) = \int \langle\psi|\mathcal{U}^\dagger\Lambda(|\psi\rangle\langle\psi|)\mathcal{U}|\psi\rangle d\mu(\psi)$, where $d\mu(\psi)$ is an average over random unitaries according to the Harr measure [57], and Λ and \mathcal{U} are experimental MTMs to be distinguished. The experimental average fidelity is 0.355 (theoretical value 0.387). Both results demonstrate that the Abelian and non-Abelian TOs have been unambiguously distinguished by their MTM ST^{-1} .

To quantify the noise levels, we calculate the average fidelity between the theoretical and experimental ST^{-1} matrices for each TO. The fidelity is $97.40\% \pm 0.78\%$ for the toric code and $98.11\% \pm 0.47\%$ for the doubled Fibonacci order. The error is around 2%, which mainly originates from the decoherence and imprecision of the real pulses. Assuming that the environment is Markovian and the dephasing noise is independent for different qubits, we numerically simulate the error propagation by solving the master equation. The simulation is in a sequence of two steps: Evolving the system by $e^{-i\mathcal{H}\Delta t}$ and subsequently dephasing for Δt , where \mathcal{H} is the total Hamiltonian including the internal Hamiltonian in Eq. (3) and the control Hamiltonian of the shaped pulse, and Δt is chosen to match the pulse discretization [43]. The average experimental error in terms of the average fidelity is 2.10% (toric code) and 1.68% (doubled Fibonacci order). The simulated noise levels matches well with the experimental

results. The remaining minor discrepancies after accounting for these simulated errors should be attributed to the fitting errors when processing the data of spectra.

Discussion. As a very promising scheme of quantum computing, TQC requires the engineering of Hamiltonians with many-body interactions. However, the notorious difficulties in engineering such Hamiltonians compel most of the preliminary experiments to utilize a state-preparation approach [19,30–33]. Exotic properties of anyons, such as the fractional statistics or path independence, have been demonstrated in diverse quantum systems. These experiments account for the Abelian toric code only. However, universal TQC requires the manipulation of non-Abelian TOs, where the simplest candidate is the doubled Fibonacci order in the string-net model. Before this work, there is no general framework to efficiently identify TOs. We introduce a quantum scattering circuit to resolve this issue, in which only single-Pauli measurements on a probe qubit are needed. As each matrix element can be directly measured, this approach provides an efficient route to reconstruct the MTMs and thus enables a polynomial scaling with the GSD. To show its generality, we perform 17-qubit numerical simulations to emulate the toric code model in square lattices, where S and T matrices are independently measured using the scattering

circuit [43]. Our experimental demonstration is carried out on a mature platform for quantum simulation tasks. Both the Abelian and non-Abelian TOs have been emulated and distinguished in a highly precise way. We anticipate our approach and corresponding experiments to trigger a wave of experimental studies in non-Abelian TOs under state-of-the-art techniques.

This work is supported by the National Key Research and Development Program of China (Grant No. 2019YFA0308100), the National Natural Science Foundation of China (Grants No. 12075110, No. 11975117, No. 11905099, No. 11875159, No. 11905111, and No. U1801661), the Guangdong Basic and Applied Basic Research Foundation (Grant No. 2019A1515011383), the Guangdong International Collaboration Program (Grant No. 2020A0505100001), the Science, Technology and Innovation Commission of Shenzhen Municipality (Grants No. ZDSYS20190902092905285, No. KQTD20190929173815000, No. JCYJ20200109140803865, and No. JCYJ20180302174036418), the Pengcheng Scholars, Guangdong Innovative and Entrepreneurial Research Team Program (Grant No. 2019ZT08C044), and Guangdong Provincial Key Laboratory (Grant No.2019B121203002).

-
- [1] D. C. Tsui, H. L. Stormer, and A. C. Gossard, *Phys. Rev. Lett.* **48**, 1559 (1982).
- [2] X. G. Wen, *Int. J. Mod. Phys. B* **04**, 239 (1990).
- [3] X. G. Wen and Q. Niu, *Phys. Rev. B* **41**, 9377 (1990).
- [4] X. Wen and A. Zee, *Nucl. Phys. B: Proc. Suppl.* **15**, 135 (1990).
- [5] X. G. Wen, *Int. J. Mod. Phys. B* **05**, 1641 (1991).
- [6] A. Kitaev, *Ann. Phys.* **321**, 2 (2006).
- [7] X. Chen, Z.-C. Gu, Z.-X. Liu, and X.-G. Wen, *Science* **338**, 1604 (2012).
- [8] M. H. Freedman, A. Kitaev, M. J. Larsen, and Z. Wang, *Bull. Am. Math. Soc.* **40**, 31 (2003).
- [9] A. Kitaev, *Ann. Phys.* **303**, 2 (2003).
- [10] S. Das Sarma, M. Freedman, and C. Nayak, *Phys. Rev. Lett.* **94**, 166802 (2005).
- [11] C. Nayak, S. H. Simon, A. Stern, M. Freedman, and S. Das Sarma, *Rev. Mod. Phys.* **80**, 1083 (2008).
- [12] E. Dennis, A. Kitaev, A. Landahl, and J. Preskill, *J. Math. Phys.* **43**, 4452 (2002).
- [13] B. M. Terhal, *Rev. Mod. Phys.* **87**, 307 (2015).
- [14] S. B. Bravyi and A. Y. Kitaev, [arXiv:quant-ph/9811052](https://arxiv.org/abs/quant-ph/9811052).
- [15] H. Zhang, C.-X. Liu, S. Gazibegovic, D. Xu, J. A. Logan, G. Wang, N. Van Loo, J. D. Bommer, M. W. De Moor, D. Car *et al.*, *Nature (London)* **556**, 74 (2018).
- [16] H. Zhang, C.-X. Liu, S. Gazibegovic, D. Xu, J. A. Logan, G. Wang, N. van Loo, J. D. Bommer, M. W. de Moor, D. Car *et al.*, *Nature (London)* **591**, E30 (2021).
- [17] M. Levin and X.-G. Wen, *Phys. Rev. Lett.* **96**, 110405 (2006).
- [18] X.-G. Wen, *Rev. Mod. Phys.* **89**, 041004 (2017).
- [19] Y.-J. Han, R. Raussendorf, and L.-M. Duan, *Phys. Rev. Lett.* **98**, 150404 (2007).
- [20] E. Rowell, R. Stong, and Z. Wang, *Commun. Math. Phys.* **292**, 343 (2009).
- [21] X.-G. Wen, [arXiv:1212.5121](https://arxiv.org/abs/1212.5121).
- [22] Y. Zhang, T. Grover, A. Turner, M. Oshikawa, and A. Vishwanath, *Phys. Rev. B* **85**, 235151 (2012).
- [23] L. Cincio and G. Vidal, *Phys. Rev. Lett.* **110**, 067208 (2013).
- [24] F. Liu, Z. Wang, Y.-Z. You, and X.-G. Wen, [arXiv:1303.0829](https://arxiv.org/abs/1303.0829).
- [25] S. Jiang, A. Mesaros, and Y. Ran, *Phys. Rev. X* **4**, 031048 (2014).
- [26] J.-W. Mei, J.-Y. Chen, H. He, and X.-G. Wen, *Phys. Rev. B* **95**, 235107 (2017).
- [27] K. Li, Y. Wan, L.-Y. Hung, T. Lan, G. Long, D. Lu, B. Zeng, and R. Laflamme, *Phys. Rev. Lett.* **118**, 080502 (2017).
- [28] M. A. Levin and X.-G. Wen, *Phys. Rev. B* **71**, 045110 (2005).
- [29] Y. Hu, S. D. Stirling, and Y.-S. Wu, *Phys. Rev. B* **85**, 075107 (2012).
- [30] C.-Y. Lu, W.-B. Gao, O. Gühne, X.-Q. Zhou, Z.-B. Chen, and J.-W. Pan, *Phys. Rev. Lett.* **102**, 030502 (2009).
- [31] G. Feng, G. Long, and R. Laflamme, *Phys. Rev. A* **88**, 022305 (2013).
- [32] A. J. Park, E. McKay, D. Lu, and R. Laflamme, *New J. Phys.* **18**, 043043 (2016).
- [33] Y.-J. Hai, Z. Zhang, H. Zheng, L. Kong, J. Wu, and D. Yu, [arXiv:2005.03236](https://arxiv.org/abs/2005.03236).
- [34] Y. P. Zhong, D. Xu, P. Wang, C. Song, Q. J. Guo, W. X. Liu, K. Xu, B. X. Xia, C.-Y. Lu, S. Han, J.-W. Pan, and H. Wang, *Phys. Rev. Lett.* **117**, 110501 (2016).
- [35] Z. Luo, J. Li, Z. Li, L.-Y. Hung, Y. Wan, X. Peng, and J. Du, *Nat. Phys.* **14**, 160 (2018).
- [36] H.-N. Dai, B. Yang, A. Reingruber, H. Sun, X.-F. Xu, Y.-A. Chen, Z.-S. Yuan, and J.-W. Pan, *Nat. Phys.* **13**, 1195 (2017).
- [37] C. K. Andersen, A. Remm, S. Lazar, S. Krinner, N. Lacroix, G. J. Norris, M. Gabureac, C. Eichler, and A. Wallraff, *Nat. Phys.* **16**, 875 (2020).

- [38] A. Erhard, H. P. Nautrup, M. Meth, L. Postler, R. Stricker, M. Stadler, V. Negnevitsky, M. Ringbauer, P. Schindler, H. J. Briegel *et al.*, *Nature (London)* **589**, 220 (2021).
- [39] K. J. Satzinger, Y.-J. Liu, A. Smith, C. Knapp, M. Newman, C. Jones, Z. Chen, C. Quintana, X. Mi *et al.*, *Science* **374**, 1237 (2021).
- [40] E. Knill and R. Laflamme, *Phys. Rev. Lett.* **81**, 5672 (1998).
- [41] C. Miquel, J. P. Paz, M. Saraceno, E. Knill, R. Laflamme, and C. Negrevergne, *Nature (London)* **418**, 59 (2002).
- [42] L.-Y. Hung and Y. Wan, *Phys. Rev. B* **86**, 235132 (2012).
- [43] See Supplemental Material at <http://link.aps.org/supplemental/10.1103/PhysRevA.105.L030402> for the complete description of the theory, experimental details, and numerical simulations, which includes Refs. [58–63].
- [44] P. Etingof, S. Gelaki, D. Nikshych, and V. Ostrik, *Tensor Categories* (American Mathematical Society, Providence, 2016), Vol. 205.
- [45] I. Cong, M. Cheng, and Z. Wang, *Phys. Rev. Lett.* **119**, 170504 (2017).
- [46] R. Cleve, A. Ekert, C. Macchiavello, and M. Mosca, *Proc. R. Soc. London, Ser. A* **454**, 339 (1998).
- [47] A. Barenco, C. H. Bennett, R. Cleve, D. P. DiVincenzo, N. Margolus, P. Shor, T. Sleator, J. A. Smolin, and H. Weinfurter, *Phys. Rev. A* **52**, 3457 (1995).
- [48] D. S. Abrams and S. Lloyd, *Phys. Rev. Lett.* **83**, 5162 (1999).
- [49] G. Passante, O. Moussa, C. A. Ryan, and R. Laflamme, *Phys. Rev. Lett.* **103**, 250501 (2009).
- [50] A. Z. Khoury, A. M. Souza, L. E. Oxman, I. Roditi, R. S. Sarthour, and I. S. Oliveira, *Phys. Rev. A* **97**, 042343 (2018).
- [51] F. A. Vind, A. Foerster, I. S. Oliveira, R. S. Sarthour, D. d. O. Soares-Pinto, A. M. d. Souza, and I. Roditi, *Sci. Rep.* **6**, 20789 (2016).
- [52] X. Nie, Z. Zhang, X. Zhao, T. Xin, D. Lu, and J. Li, [arXiv:1903.12237](https://arxiv.org/abs/1903.12237).
- [53] X. Nie, B.-B. Wei, X. Chen, Z. Zhang, X. Zhao, C. Qiu, Y. Tian, Y. Ji, T. Xin, D. Lu, and J. Li, *Phys. Rev. Lett.* **124**, 250601 (2020).
- [54] X. Nie, X. Zhu, C. Xi, X. Long, Z. Lin, Y. Tian, C. Qiu, X. Yang, Y. Dong, J. Li, T. Xin, and D. Lu, [arXiv:2011.12580](https://arxiv.org/abs/2011.12580).
- [55] C. A. Ryan, C. Negrevergne, M. Laforest, E. Knill, and R. Laflamme, *Phys. Rev. A* **78**, 012328 (2008).
- [56] N. Khaneja, T. Reiss, C. Kehlet, T. Schulte-Herbrüggen, and S. J. Glaser, *J. Magn. Reson.* **172**, 296 (2005).
- [57] J. Emerson, R. Alicki, and K. Życzkowski, *J. Opt. B: Quantum Semiclass. Opt.* **7**, S347 (2005).
- [58] T. Lan and X.-G. Wen, *Phys. Rev. B* **90**, 115119 (2014).
- [59] N. E. Bonesteel, L. Hormozi, G. Zikos, and S. H. Simon, *Phys. Rev. Lett.* **95**, 140503 (2005).
- [60] D. Lu, K. Li, J. Li, H. Katiyar, A. J. Park, G. Feng, T. Xin, H. Li, G. Long, A. Brodutch, J. Baugh, B. Zeng, and R. Laflamme, *npj Quantum Inf.* **3**, 45(2017).
- [61] C. Negrevergne, R. Somma, G. Ortiz, E. Knill, and R. Laflamme, *Phys. Rev. A* **71**, 032344 (2005).
- [62] C. Raitz, A. M. Souza, R. Auccaise, R. S. Sarthour, and I. S. Oliveira, *Quantum Inf. Process.* **14**, 37 (2015).
- [63] A. M. Souza, I. S. Oliveira, and R. S. Sarthour, *New J. Phys.* **13**, 053023 (2011).